From molecular spectroscopy to entanglement of atoms – a trek with supersonic velocity

Jarosław KOPERSKI

Smoluchowski Institute of Physics, Jagiellonian University,
Reymonta 4, 30-059 Kraków, Poland;
e-mail: ufkopers@cyf-kr.edu.pl

The supersonic free-jet expansion technique is being used in different fields of research in physics, and physical chemistry to study vibrational and rotational molecular structures in ground and excited electronic energy states. The supersonic beam technique exploits a source of monokinetic, rotationally and vibrationally cold van der Waals (vdW) molecules that are very weakly bound in their ground electronic states. In this article we review experiments at the Jagiellonian University in Kraków (Poland) in which the supersonic free-jet beam serves as a source of ground-state vdW molecules in studies of neutral–neutral interactions between 12-group metal (Me = Zn, Cd, Hg) and 18-group noble gas (Ng = He, Ne, Ar, Kr, Xe) atoms. The experiments lead to determination of spectroscopical characteristics and interatomic potentials of MeNg and Me_2 molecules, allowing determination of distinct trends in the Me–Ng and Me–Me interactions in different regions of internuclear separation. The determined interatomic potentials are also used in designing mechanisms of internal vibrational cooling of molecules photoassociated in magneto-optical traps. Recently, versatility of supersonic beams is confirmed in quantum information where the technique is planned to be used to create pairs of entangled atoms in experiments dedicated for testing of Bell's inequality for atoms. A purpose of the experiment – which is in a preparational stage in our laboratory – is to create pairs of entangled cadmium atoms with regard to their nuclear spin orientations. It is planned to be achieved in supersonic molecular beams of cadmium dimers using two dye-laser pulses and stimulated Raman process leading to a controlled photodissociation of the molecule.

Keywords: supersonic free-jet expansion, cooling of molecules, van der Waals molecules, interatomic potentials, covalent admixture, dissociation energy, bond length, vibrational energy, rotational energy, entanglement of atoms, Bell inequality.

1. Introduction

The van der Waals (vdW) forces [1] are responsible for many phenomena such as atom–surface interaction, diffusion, adsorption, adhesion, liquids flow, solvolysis, and viscosity. They dominate in liquids, molecular crystals, polymers and biological systems resulting in their structural properties, for example, they play a fundamental role in the stability and conformation of biomolecules such as DNA and RNA, proteins

and their complexes. The vdW forces are important from the point of view of searching for new technologies (they allow condensing gases as well as permitting, *e.g.*, to use graphite as a lubricant) or for new materials, *e.g.*, so-called *gecko-tapes* [2]. The properties of small vdW clusters, of which dimers are the simplest prototypes, are of current interest with an eye towards the understanding forces that hold liquids and solids together as well as transition of molecular properties to bulk metal properties [3, 4]. Consequently, these are the vdW dimers that are of current interest. They represent a unique class of simple heteronuclear and homonuclear diatomic species with very small (10–1000 cm^{-1}) dissociation energies, thus filling some of the last gaps in a periodic table of dimers [5]. Experimental determination of the unusual vdW nature of these species provides a good test for theoretical formulations [6] which aid our understanding of simple models as well as phenomenological regularities that govern the long-range dispersion forces (*i.e.*, London–Drude theory [7, 8], Slater–Kirkwood [9] and Kramer–Herschbach [10] models, or Liuti–Pirani [11] and Tang–Toennies [12] regularities). Determination and understanding of simple vdW forces mechanism in elementary diatoms enable to build a picture of binding in larger complexes of this type (*e.g.*, [13–15]). This bridges the gap between the vdW molecules and clusters. The electronic properties of excimers and exciplexes allow a relatively easy production of population inversions, thus making them likely candidates for laser media [16, 17]. In different branches of atomic and molecular physics there is rapidly growing interest in long-range forces acting between atoms which interact in a variety of traps, experiments of matter-wave interferometry, photoassociation of cold molecules [18], quantum degeneracy, quantum entanglement from dissociation of diatomic molecules [19, 20], and internal vibrational cooling of molecules [21]. Recently, the interest in highly-excited (Rydberg) molecular electronic states has been revived in the context of two- and three-step photoassociation processes in magneto-optical traps [22, 23]. Knowledge of the complex shape of the Rydberg-state interatomic potential allows designing the photoassociation schemes for molecules and makes the cooling processes highly efficient.

The London dispersion vdW-type interaction* acts between two induced electric dipole moments created in, *e.g.*, two neutral atoms, and dominates the long-range tail of diatomic molecular potential if the two atoms forming the molecule are in S electronic energy state (*e.g.*, Me(n^1S_0) + Me(n^1S_0)). If the atoms are sufficiently far apart that their electron clouds overlap is negligible, the interatomic potential in the long-range region can be written as:

$$U(R) \ = \ D_e - \sum_{k=3}^{\infty} \frac{C_{2k}}{R^{2k}} \ = \ D_e - \left(\frac{C_6}{R^6} + \frac{C_8}{R^8} + \frac{C_{10}}{R^{10}} + \ldots \right) \tag{1}$$

*The other two vdW-type interactions, *i.e.*, Keesom and Debye, are those acting between two permanent electric dipole moments, and between permanent and induced dipole moments, respectively.

where D_e is the dissociation energy limit. For large R, one power of R will usually dominate and the potential can be approximated as $U(R) = D_e - C_m/R^m$, where m is in general not an integer, and $m = 6$ for pure vdW interaction ($m = 8$ for dipole–quadrupole, $m = 10$ for quadrupole–quadrupole and dipole–octupole, *etc*., interactions). Although at large R only the leading term makes a substantial contribution to the attractive energy, at smaller R near to equilibrium internuclear separation R_e, it is found [24] that the higher order terms may contribute as much as 20% of the total dispersion energy.

The interaction of closed-shell (neutral) metal (Me) or noble gas (Ng) atom with ground- or electronically excited-state Me atom is an example of vdW interaction, and it has been an important area of study in our laboratory [25–42]. The studied complexes consist of 12-group Me (Zn, Cd, Hg) homoatomic Me_2 as well as 12-group and 18-group Ng (He, Ne, Ar, Kr, Xe) heteroatomic MeNg complexes. Determination of accurate interatomic potentials for specific Me_2 or MeNg ground and excited-state interactions in different regions of internuclear separation is important to broaden our knowledge about these basic interactions. A special emphasis has been placed on searching for an evidence of a covalent admixture to the vdW bonding [43] as well as explaining irregularities (*i.e.*, double-well potentials, potential barriers) in the excited--state interatomic potentials. The experimentally derived interatomic potentials are frequently confronted against results of *ab initio* calculations.

2. Experimental method

2.1. Supersonic free-jet expansion

Over the past several decades physicists have learned to translationally cool atoms to very low temperatures using properly arranged laser beams coupled to closed resonance transitions. The payoffs have included atom interferometry, precision spectroscopy, atomic Bose–Einstein condensates (BEC), beams of coherent matter (so-called atom lasers) and studies of the interactions between ultra-cold atoms (cold and ultra--cold for atoms or molecules at $T_t < 1$ K and $T_t < 1$ mK, respectively [44], where T_t is a translational temperature). The obvious next step would be an extension of the approach to more complex objects–molecules. Unfortunately, the same approach does not work due to the multitude of fluorescence paths via ro-vibrational bound–bound as well as bound–free transitions that are available after a selective ro-vibrational excitation in a molecule. This obstacle has led to a growth in the number of methods to not only achieve an effective translational cooling of molecules but to also provide control over rotational and vibrational degrees of freedom.

Supersonic free-jet expansion technique is a widely used method in laser spectroscopy of molecules. The method has been engaged in different fields of research in physics, chemistry and in both physical chemistry and chemical physics. The supersonic expansion technique provides a source of *rotationally and*
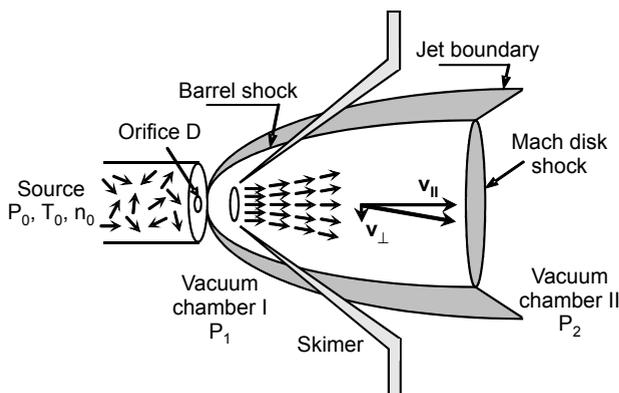
Fig. 1. Schematic cross-section of a supersonic free-jet expansion beam. P_0, T_0, n_0 – pressure, temperature, and density of expanding species in the source, respectively; D – diameter of the orifice; P_1 – background pressure ($P_1 \ll P_0$). Arrows show the thermal and ordered movement of expanding species behind and downstream from the nozzle, respectively. Translational $\mathbf{v}_{||}$ and transverse $\mathbf{v}_\perp$ components of the resulting velocity $\mathbf{v}$ of the expanding species are shown. Thanks to the adiabatic process in the orifice, along the expansion a narrowing of the translational velocity distribution $N(\mathbf{v}_{||})$ occurs relatively to the modified Maxwell distribution $N(\mathbf{v}_{||}) \propto \exp[-m(\mathbf{v}_{||} - \mathbf{u})^2/2kT_{||}]$, where $\mathbf{u}$ and m are the mean translational velocity of the gas in the beam and the mass of the expanding species. Beams discussed here are *supersonic free-jet expansion beams* in which the expanded medium leaves the reservoir through an orifice and undergoes wall-free expansion into the vacuum; another category is the *supersonic nozzle expansion beam* in which a conically shaped aperture – a skimmer, shown for reference – eliminates jet boundaries and leaves only a central well defined part of the beam. The molecular beam apparatus with supersonic nozzle expansion is presently developed in our laboratory (see Section 2.3).

vibrationally cold molecules, which are *very weakly bound* in their ground electronic states (*e.g.*, CdHe dissociation energy $D_e'' = 14.2$ cm^{-1} [26]). Moreover, in a certain part of the expansion called *zone of silence* the molecules can be treated as *isolated* objects that are *travelling* in the beam without collisions.

When a gas of Me atoms and Me$_2$ molecules mixed with a carrier Ng* expands freely from a high-pressure region (P_0) through a small orifice with diameter D into the vacuum (P_1) (refer to Fig. 1 and to [21]), an adiabatic cooling of the internal energy occurs. During the process, the thermal energy of the molecules in the source is partly transferred into the expansion energy. In the source, the thermal energy is comprised of translational, vibrational and rotational energies (temperatures), and $T_0 = (T_{||} = T_\perp) = T_v = T_r$, where T_0 is the temperature in the source, $T_{||}$ and $T_\perp$ are translational and transverse temperatures, and T_v and T_r are vibrational and rotational temperatures in the beam, respectively. The energy transfer takes place in the orifice at densities where the collision probability is very high and $\lambda_0 \ll D$, where λ_0 is a mean free path of the expanding gas. The degree of cooling depends on the number of

---

*Here one considers two-component supersonic beams in which a special class is represented by seeded molecular beams (the seeded gas, *e.g.*, Me vapor, has a much smaller density number than the Ng carrier at P_0, *i.e.*, $n_{Me} \ll n_{Ng}$).

collisions during the expansion, which is proportional to $n_0 D$, where n_0 is the density of the expanding species in the source and its orifice [45]. In the expansion, the translational cooling (monokinetization, *i.e.*, narrowing of the translational velocity distribution $N(\mathbf{v}_{||})$) is more effective than the rotational or vibrational cooling, and after the adiabatic expansion $T_\perp < T_{||} < T_r < T_v$. Terminal translational temperature, $T_{||\infty}$, in the free-jet beam can be estimated using formula which was derived for Ar as the carrier gas [46]:

$$T_{||\infty} \approx \frac{T_0}{1 + 5896(P_0 D)^{0.8}} \tag{2}$$

where T_0, P_0 and D are expressed in K, atm and cm, respectively. For typical conditions of the continuous free-jet expansion in experiments in our laboratory ($T_0 = 900$ K, $P_0(\text{Ar}) = 11$ atm, $D = 0.02$ cm) one can approximate $T_{||\infty} \approx 510$ mK. Usually, one assumes $T_r \approx T_{||\infty}$ and T_v as about one order of magnitude higher that T_r [25]. It was reported that in the central part of the expansion $T_{||}$ can decrease to 1–30 mK, particularly when He is used as a carrier gas [45]; $T_\perp$ can even decrease to 0.5–10 mK. The results presented here were obtained using continuous (Me = Cd or Zn seeded in Ng = Ne, Ar, Kr or Xe) supersonic free-jet beam. Typical T_r and T_v attainable in the beam were estimated to be 0.5–3 K and 5–30 K, respectively.

2.2. Laser spectroscopy in supersonic beam

Laser-induced *excitation spectra* are produced by scanning the laser frequency over the structure of the excited electronic energy state (isotopic, vibrational, rotational) while recording the total fluorescence signal. Using the supersonic free-jet expansion one simplifies the spectra as the excitation starts mostly from the lowest vibrational and rotational levels of the ground electronic energy state. Using excitation spectra, the energy structure in the excited-state bound well can be investigated (bound ← bound transitions) even up to the dissociation limit if allowed by the "Franck–Condon (F-C) window" for the excitation (see [27, 29, 30, 33, 39, 40]). In some cases (free ← bound transitions) permit determination of a shape of the repulsive part in the excited-state potential (see [28, 34, 36]) as well as position and shape of the excited-state potential barrier (see [31, 35, 41]).

Laser-induced *fluorescence spectra* (called also *dispersed emission spectra*), which occur after a selective excitation of a ro-vibrational level in the excited state, may terminate at different parts of the ground-state interatomic potential. From one point of view (bound → free transitions), it makes possible an accurate determination of steepness of the ground-state repulsive part and, consequently, it allows description of a short-range interaction between atoms constituting the molecule providing possibility for estimation of a *covalent admixture* to the ground-state vdW bonding [26]. Characterization of such a kind has been performed in our laboratory for a number of complexes such as Cd_2 [27, 31], as well as ZnNe, ZnAr and ZnKr [38]. From the other side (bound → bound transitions), using dispersed emission spectra, the energy struc-

ture in the ground-state bound well can also be investigated extending the ground-state characterization well above the lowest ro-vibrational levels. Using this approach, the vibrational structure of the ground state of Cd_2 [39], Zn_2 [42] and ZnNg [38] has been studied.

2.3. New experimental set-up at the Jagiellonian University

The experimental set-up that was previously used in our laboratory consisted of a vacuum expansion chamber equipped with *continuously* operated stainless-steel (or molybdenum) high-temperature supersonic free-jet beam source. The set-up was described earlier in a number of articles [25–42] and was extensively used over fifteen years. In order to make an improvement and to alter the set-up (to meet our present requirements for the *proposed* experiment (*i.e.*, generation of entangled atoms from diatomic molecules [41])), new complex apparatus consisting of four vacuum chambers was built [47]. It accommodates specifically designed high-temperature *pulsed* stainless-steel beam source. The quality of the expansion was improved by placing a skimmer between the chamber with the beam source and that devoted to molecular spectroscopy and production of entangled atoms.

Excitation and fluorescence spectra were produced using a number of pulsed lasers, mainly Nd:YAG-pumped dye lasers, with spectral bandwidth varying between 0.05 cm^{-1} and 1 cm^{-1}. The dye lasers were equipped with frequency doubling generators in order to provide the excitation radiation in the UV spectral region. After excitation the total fluorescence signal was recorded using photomultiplier tubes (PMT) (*e.g.*, [28–30, 33, 34, 36, 37, 40, 41]). Analysis of the fluorescence spectra was performed using various wavelength-scanned monochromators (*e.g.*, [27, 35]) or spectrographs (*e.g.*, [38, 39]) equipped with PMT or CCD camera, respectively. In the case of the fluorescence spectra the spectral resolution of the detection system approached 1 cm^{-1} or 13 cm^{-1}, respectively, and in certain cases did allow resolving the bound $\rightarrow$ bound transitions (*e.g.*, [39]).

3. Spectra

3.1. Excitation spectra

Laser induced fluorescence (LIF) excitation spectrum is shown in Fig. 2. It presents rotational profile of the $^{228}Cd_2$ isotopologue in $(v', v'') = (26, 0)$ vibrational band of the $A^1 0_u^+(5\,^1P_1) \leftarrow X^1 0_g^+$ transition. The profile is simulated assuming full isotopic composition of the $^{228}Cd_2$ isotopologue. The simulation allowed first-time determination of the $B'_e(A^1 0_u^+) = 0.040(2)$ cm^{-1} and $B''_e = 0.0209(5)$ cm^{-1} rotational constants, and the $R'_e(A 0_u^+) = 2.71(7)$ Å and $R''_e = 3.76(4)$ Å bond lengths of the excited and ground states, respectively. Moreover, the obtained absolute value for Cd_2 ground-state bond length was smaller than the $R''_e = 4.58$ Å predicted from a pure vdW interaction but closer to the *ab initio* values $R''_e = 3.98$ Å [27] and 3.915 Å [49].
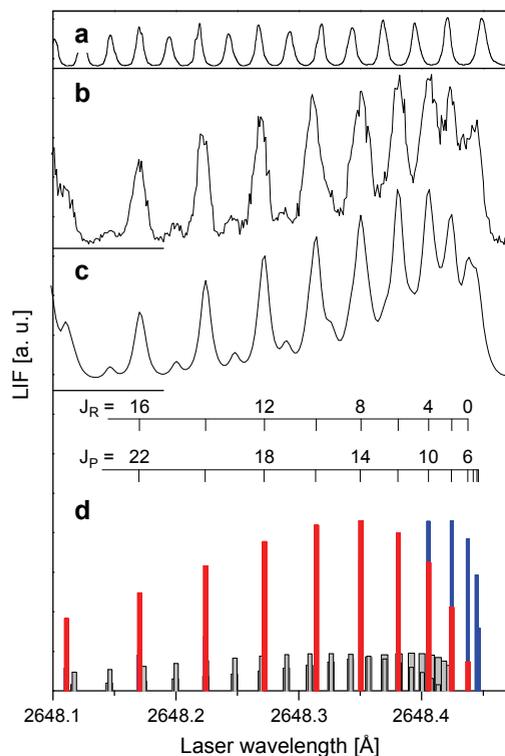
Fig. 2. Rotational profile of $^{228}Cd_2$ isotopologue recorded in $(v', v'') = (26, 0)$ vibrational band of the $A0_u^+(5\,^1P_1) \leftarrow X0_g^+(5\,^1S_0)$ transition. (**b**) Experimental trace; (**c**) computer simulated [48] profile obtained as a result of convolution of every rotational transition with a Voigt function; in the simulations $\Delta_{las} \approx 0.08$ cm^{-1}, $\Delta_{Dopp} \approx 0.12$ cm^{-1} and rotational temperature $T_r = 13$ K were assumed; (**d**) *P*-branch (blue bars) and *R*-branch (red bars) of the $(^{114}Cd)_2$ isotopologue; *P*- and *R*-branches of the $^{112}Cd\,^{116}Cd$ isotopologue (grey bars). (**a**) Fringes recorded using a Fabry–Perot etalon (FSR = 0.2 cm^{-1}) for a fundamental dye-laser frequency.

Our result indicates that the hypothesis of a covalent admixture is plausible. Consequently, the ground-state bonding in group-12 Me$_2$ molecules (particularly in Cd$_2$ but also in Hg$_2$ [51]) cannot be described as pure vdW interaction.

3.2. Dispersed emission spectra

Laser induced fluorescence (LIF) dispersed emission spectrum is shown in Fig. 3. It presents characteristic Condon internal diffraction (CID) pattern recorded for ZnKr using the $C^1\Pi_1(4\,^1P_1) \to X^1\Sigma_0^+(4\,^1S_0)$ transition after a selective excitation of the $v' = 19$ level. The simple oscillatory pattern suggests their reflection rather than interference structure [52]. The CID pattern continues into the bound $\to$ bound part of the spectrum (most short-wavelength part of trace **b**) in the form of the F-C factors envelope of the discrete transitions. The experimental profiles are result of integration
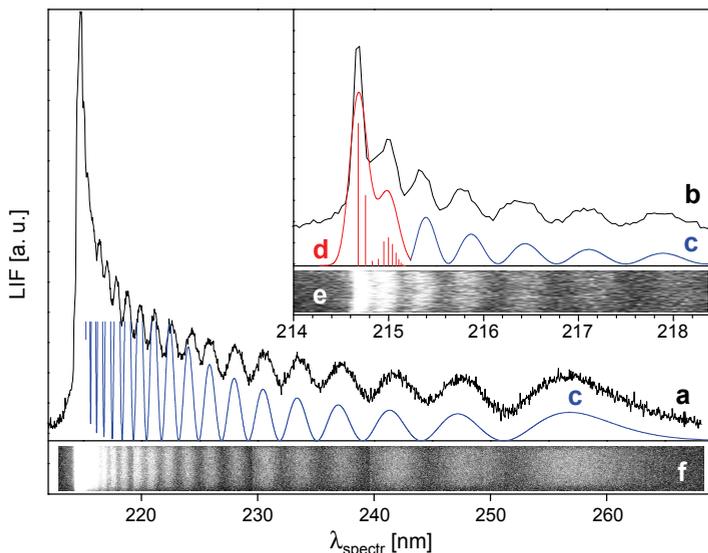
Fig. 3. LIF dispersed emission spectrum of ZnKr recorded using the $C^1\Pi_1(4\,^1P_1) \to X^1\Sigma_0^+(4\,^1S_0)$ transition after a selective excitation of the $v' = 19$ level. (**a**) Gross and (**b**) most short-wavelength part of the spectrum recorded with 100 cm^{-1} and 30 cm^{-1} spectral resolution, respectively. (**c**) Simulation [50] of the bound $\to$ free part (blue line) performed with an assumption that the $C^1\Pi_1$ and repulsive part of the $X^1\Sigma_0^+$ state potentials are represented with Morse and Maitland–Smith M-S($n_0 = 9.09$, $n_1 = 7.81$) [26] functions, respectively (amplitudes of the first five bound $\to$ free maxima were saturated). Simulated most short-wavelength part of the spectrum, includes (**c**) as above (blue line), and (**d**) bound $\to$ bound transitions (F-C factors represented with red vertical lines). The individual F-C factors corresponding to the $v' = 19 \to v''$ vibrational transitions were convoluted with a Gaussian function (FWHM = 30 cm^{-1}) representing the spectrograph throughput. (**e**) and (**f**) pictures from a CCD camera corresponding to (**a**) and (**b**), respectively, showing a shape of the $v' = 19$ wave-function squared.

of a signal extracted from the CCD camera images (traces (**e**) and (**f**), respectively), showing a shape of the $v' = 19$ vibrational wave-function squared – real snapshots from the *molecular quantum world*. The number of maxima in the spectrum is equal to $v' + 1$, which is frequently used to corroborate the assignment in the $C^1\Pi_1 \leftarrow X^1\Sigma_0^+$, $v'' = 0$ excitation spectrum reported in [34]. Due to the limited resolution of the detection system it was not possible to resolve the $v' \to v''$ bound–bound transitions (shown in Fig. 3**d** with red vertical lines). Increasing to higher v'' values and passing through the $X^1\Sigma_0^+$ state dissociation limit, the unresolved $v' \to v''$ components smoothly transform into the continuous spectra of the bound $\to$ free transitions, forming the gross CID pattern. The main objective of the investigation was determination of the repulsive part of the $X^1\Sigma_0^+$-state potential of ZnKr. The best was the representation using a Maitland–Smith, M-S(n_0, n_1), function [26] which is a Lennard–Jones, L-J($n - 6$) potential, with the parameter n being a function of R, $\tilde{n} = n_0 + n_1(R/R_e'' - 1)$. The M-S($n_0$, n_1) potential was successfully applied to represent the ground-state interatomic potential the ZnAr, CdAr, HgAr, CdKr and HgKr [25].

4. Interatomic potentials

4.1. Excited-state potentials

One of the objectives of the studies performed in Kraków's group was explanation of irregularities (*i.e.*, double-well potentials, potential barriers) in the excited state interatomic potentials. It was achieved by recording, analyzing and simulating bound ← bound and free ← bound LIF excitation spectra for the CdKr [53], Cd$_2$ [35] and CdNg (Ng = Ne, Ar, Kr) [54–56] molecules and determining the double-well structure of the $B^31(5^3P_1)$, $B^11_u(5^1P_1)$ and $E^3\Sigma_1^+(6^3S_1)$ potentials, respectively. In case of the $E^3\Sigma_1^+$ Rydberg-state potentials, the excitation was achieved using the optical–optical double resonance method via two $A^30^+(5^3P_1)$ and $B^31(5^3P_1)$ intermediate electronic states with considerably different R'_e (*i.e.*, $R'_e(A^30^+) <$ $< R'_e(B^31)$) to explore in a relatively large interval of R in the complex structure of the $E^3\Sigma_1^+$-state potential. In case of the B^31 and B^11_u potentials of CdKr and Cd$_2$, respectively, in order to define accurate potential energy curves, an inverted perturbation approach (IPA) method [57] was applied to the experimentally measured energies of vibrational levels in different isotopologues (see Fig. 4).

4.2. Ground-state potentials

The postulated covalent admixture to the ground-state vdW bonding (see Sections 1.1 and 2.2) can have impact on the magnitude of the bond length. For 12-group
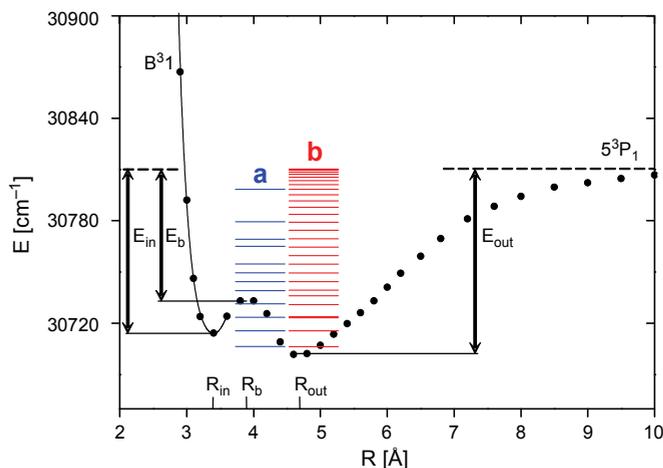
Fig. 4. The double-well $B^31(5^3P_1)$-state potential of CdKr (full circles approximated with spline function (solid line)) found as a result of calculation based on the inverted perturbation approach (IPA) method [57] using energies recorded in the experiment as input data. (**a**) Energies of the vibrational levels recorded in the experiment and (**b**) eigenvalues generated for finally obtained B^31-state potential. Positions of outer and inner minima, E_{out} = 109.2 cm^{-1}, R_{out} = 4.70 Å, E_{in} = 96.8 cm^{-1}, R_{in} = 3.36 Å, and potential barrier, E_b = 77.6 cm^{-1}, R_b = 3.89 Å, are shown.

homoatomic dimers (Hg$_2$, Zn$_2$, Cd$_2$), values of R''_e calculated from the pure London dispersion relation described with Eq. (1) increase (4.01 Å, 4.35 Å, 4.58 Å, respectively) as static dipole polarizability α_M increases (5.02 Å^3, 5.75 Å^3, 7.36 Å^3, respectively) and are evidently larger than those obtained from *ab initio* calculations of DOLG and co-workers (3.73 Å, 3.88 Å, 4.05 Å, respectively) [58, 59] in which it was explicitly assumed that one-fourth of the ground-state bonding is a non-dispersion-like covalent bonding. The experimental values (3.654 Å [51], 4.19 Å [29], 3.76 Å [33], respectively), except that for Zn$_2$, seem to confirm the character of the bonding. However, only those for Hg$_2$ [51] and Cd$_2$ [33] were determined using low-resolution rotational spectroscopy. The ground-state bond length for Zn$_2$ was only investigated in an experiment with vibrational resolution [29].

5. Applications

5.1. Photoassociation, vibrational cooling and E-P-R experiment

An internal vibrational cooling is a process that can occur in a molecule by employing the $\nu' \leftrightarrow \nu''$ transitions between two electronic energy states for which ΔR_e is very small. Such a situation occurs for the $F\,^3 0^+_u (5\,^3P_1) \leftrightarrow X\,^1 0^+_g$ transition in Hg$_2$. The transition was extensively studied [60] and constitutes the basis of so-called Walther's scheme [61]. The molecule-forming process starts upon a collision of two trapped ground-state Hg atoms. Due to the 253.7 nm laser they undergo a photoassociation (PA) transition into ν' level in the $F\,^3 0^+_u$ state. A single-step PA process leaves translationally cold molecule in rather high T_ν and T_r, *i.e.*, in relatively high (ν'', J'') level. As determined in our laboratory [25], the $F\,^3 0^+_u \leftrightarrow X\,^1 0^+_g$ bound–bound transitions in Hg$_2$ (which are centred at 254.1 nm) are strongly allowed, particularly those with $\Delta \nu = \nu' - \nu'' = 0$ because of the exceptionally small $\Delta R_e = 0.030 \pm 0.002$ Å. The cooling relies on decreasing the ν'' quantum number by continuous blue detuning of the 254.1 nm laser, and successive acts of laser excitation (at $\Delta \nu = -1$ transitions) and fluorescence (at $\Delta \nu = 0$ transitions that are favoured over those at $\Delta \nu = -1$ since the former are characterized by approximately 10–40 times larger F-C factors). In addition, rotational heating does not occur during the process [21].

What is very important and deserves a great deal of attention is an investigation of long range interaction potentials of the excited and ground states of Hg$_2$ using PA spectroscopy. Hg$_2$ is important for testing new approaches to *ab-initio* calculations due to the presence of relativistic effects and correlations. These measurements may result in important input data for these models.

A sophisticated application of a supersonic expansion of dimers which is proposed and currently realized in our laboratory is associated with fundamental tests of quantum mechanics, *i.e.*, test of Bell inequality for neutral atoms. In 1995, FRY *et al.* [62] proposed a loophole-free experimental realization of Bohm's spin-1/2 particle version of the Einstein–Podolsky–Rosen (E-P-R) experiment for (^{199}Hg)$_2$. In the proposal,

photodissociation of a diatomic molecule is a critical initial step to create two atoms in an entangled state. In our laboratory we follow the idea and extend the proposal for the isotope of another 12-group atom, namely ^{111}Cd. Two ^{111}Cd atoms in the $5\,^1S_0$ state, each with nuclear spin ($I = 1/2$), are produced in an entangled state with total nuclear spin equal zero ($I_{tot} = 0$). Such a state is obtained by dissociating the (^{111}Cd)$_2$ isotopologue produced in its $X\,^1 0_g^+$ ground state in a pulsed supersonic expansion beam using two consecutive laser pulses at the $A\,^1 0_u^+ (5\,^1P_1) \leftarrow X\,^1 0_g^+$ bound–bound (257.1 nm) and $A\,^1 0_u^+ \rightarrow X\,^1 0_g^+$ free–bound (305.0 nm) transitions which constitute the so-called stimulated Raman process. The measurement of nuclear spin correlations between the two atoms in the entangled state is achieved by detection of the atoms using a spin state selective two-photon excitation–ionization scheme via the measurement of the resulting (e^-)–$(^{111}$Cd$^+)$ pairs [63]. The crucial aspect of the proposed experiment is that the ^{111}Cd atoms in a given pair are "born together" from one (^{111}Cd)$_2$ molecule which was earlier produced in a supersonic expansion beam.

5.2. *Gecko-tapes* and *waalbots*

One of the examples of practical application that comes from the studies of vdW interaction is that based on adhesive force acting between gecko foot and a surface. In 2000 AUTUMN and co-workers [64] measured for the first time the force acting between a single hair (called seta) extracted from tokay gecko's (*Gekko gecko*) foot and a glass surface. A single seta of the tokay gecko is roughly 110 µm long and 4.2 µm wide. Each of the seta's branches ends in a thin, triangular *spatula* connected at its apex. The end is about 0.2 µm long and 0.2 µm wide. AUTUMN and co-workers concluded that each seta produces an average force of 20 µN. As the foot of a gecko has about 5000 setae per mm^2, therefore it can produce 10 N of adhesive force with approximately 100 mm^2 of surface area. Consequently, the measurements indicated that if all setae were simultaneously and maximally attached, a single foot of a gecko could produce 100 N of adhesive force.

Results of the studies contributed to the invention of so-called *gecko-tapes*. In 2003 GEIM *et al*. [2] introduced a prototype of such a self-adhesive tape made by microfabrication of dense arrays of flexible plastic (polymer polyimide) pillars on a soft bonding substrate (scotch tape), the geometry of which is optimized to ensure their collective adhesion. Their approach showed a way to manufacture self-cleaning, re-attachable dry adhesives, however a problem related to their durability was not resolved. Although, the new material is still in its development stage, the *gecko-tapes* found its application in robotics [65] where Murphy and Sitti proposed a small-scale agile wall-climbing gecko-footed robot (*waalbot*) which was able to climb on smooth vertical surfaces using flat adhesive elastomer material (Vytaflex 10) for attachment. Along with their second generations of *waalbots* [66] the authors introduced autonomous adhesion recovery and a motion planning implementation which resulted in the ability to navigate to a goal in complex three-dimensional environments and

avoiding obstacles. The robots are intended for inspection and surveillance applications, and ultimately, for space missions.

References

[1] VAN DER WAALS J.D., *The equation of state for gases and liquids*, [In] *Nobel Lectures, Physics 1901–1921*, Elsevier Publishing Company, Amsterdam, 1967, pp. 254–265; MARGENAU H., *Van der Waals forces*, Reviews of Modern Physics **11**(1), 1939, pp. 1–35, and references therein.

[2] GEIM A.K., DUBONOS S.V., GRIGORIEVA I.V., NOVOSELOV K.S., ZHUKOV A.A., SHAPOVAL S.YU., *Microfabricated adhesive mimicking gecko foot-hair*, Nature Materials **2**(7), 2003, pp. 461–463.

[3] HENSEL F., *The liquid–vapour phase transition in fluid metals*, Philosophical Transactions of the Royal Society of London A **356**(1735), 1998, pp. 97–117, and references therein.

[4] MORSE M.D., *Clusters of transition-metal atoms*, Chemical Reviews **86**(6), 1986, pp. 1049–1109, and references therein.

[5] HUBER K.P., HERZBERG G., *Molecular Spectra and Molecular Structure. IV. Constants of Diatomic Molecules*, D. Van Nostrand, New York, 1979.

[6] BUCKINGHAM A.D., FOWLER P.W., HUTSON J.M., *Theoretical studies of van der Waals molecules and intermolecular forces*, Chemical Reviews **88**(6), 1988, pp. 963–988.

[7] LONDON F., *Zur Theorie und Systematik der Molekularkräfte*, Zeitschrift für Physik **63**, 1930, pp. 245–279.

[8] STONE A.J., *The Theory of Intermolecular Forces*, Clarendon, Oxford, 1996.

[9] SLATER J.C., KIRKWOOD J.G., *The van der Waals forces in gases*, Physical Review **37**(6), 1931, pp. 682–697.

[10] KRAMER H.L., HERSCHBACH D.R., *Combination rules for van der Waals force constants*, Journal of Chemical Physics **53**(7), 1970, pp. 2792–2800.

[11] LIUTI G., PIRANI F., *Regularities in van der Waals forces: correlation between the potential parameters and polarizability*, Chemical Physics Letters **122**(3), 1985, pp. 245–250.

[12] LI P., REN J., NIU N., TANG K.T., *Corresponding states principle for the alkaline earth dimers and the van der Waals potential of Ba_2*, Journal of Physical Chemistry A **115**(25), 2011, pp. 6927–6935.

[13] MARTENCHARD-BARRA S., JOUVET C., LARDEUX-DEDONDER C., SOLGADI D., *Solvation of $Hg(^3P_1)$ in the $HgAr_n$ clusters through resonant enhanced multiphoton ionization: Evidence for nonadditive effects in the excited state potentials*, Journal of Chemical Physics **98**(7), 1993, pp. 5281–5289.

[14] BRÉCHIGNAC C., BROYER M., CAHUZAC P.H., DELACRETAZ G., LABASTIE P., WÖSTE L., *Size dependence of inner-shell autoionization lines in mercury clusters*, Chemical Physics Letters **120**(6), 1985, pp. 559–563.

[15] LANG B., VIERHEILIG A., WIEDENMANN E., BUCHENAU H., GERBER G., *Multiple ionization and Coulomb explosion of mercury clusters in femtosecond laser fields*, Zeitschrift für Physik D **40**(1–4), 1997, pp. 1–4.

[16] MILLER J.C., ANDREWS L., *Absorption and laser-excited fluorescence spectra of matrix-isolated metal van der Waals dimers*, Applied Spectroscopy Reviews **16**(1), 1980, pp. 1–42, and references therein.

[17] RHODES C.K. [Ed.], *Excimer Lasers*, 2nd Ed., Springer-Verlag, 1984, and references therein.

[18] LETT P.D., JULIENNE P.S., PHILLIPS W.D., *Photoassociative spectroscopy of laser-cooled atoms*, Annual Reviews of Physical Chemistry **46**, 1995, pp. 423–452.

[19] ESQUIVEL R.O., FLORES-GALLEGOS N., MOLINA-ESPÍRITU M., PLASTINO A.R., ANGULO J.C., ANTOLÍN J., DEHESA J.S., *Quantum entanglement and the dissociation process of diatomic molecules*, Journal of Physics B: Atomic, Molecular and Optical Physics **44**(17), 2011, article 175101.

[20] CHELKOWSKI S., BANDRAUK A.D., *Visualizing electron delocalization, electron–proton correlations, and the Eistein–Podolski–Rosen paradox during the photodissociation of a diatomic molecule using two ultrashort laser pulses*, Physical Review A **81**(6), 2010, article 062101.

[21] KOPERSKI J., FRY E.S., *Molecules in the cold environment of a supersonic free-jet beam: from spectroscopy of neutral–neutral interactions to a test of Bell's inequality*, Journal of Physics B: Atomic, Molecular and Optical Physics **39**(19), 2006, pp. S1125–S1150.

[22] COMPARAT D., DRAG C., LABURTHE TOLRA B., FIORETTI A., PILLET P., CRUBELLIER A., DULIEU O., MASNOU-SEEUWS F., *Formation of cold Cs2 ground state molecules through photoassociation in the 1u pure long-range state*, The European Physical Journal D **11**(1), 2000, pp. 59–71.

[23] ALMAZOR M.-L., DULIEU O., MASNOU-SEEUWS F., BEUC R., PICHLER G., *Formation of ultracold molecules via photoassociation with blue detuned laser light*, The European Physical Journal D **15**(3), 2001, pp. 355–363.

[24] MAITLAND G.C., RIGBY M., SMITH E.B., WAKCHEM W.A., *Intermolecular Forces*, Clarendon, Oxford, 1987.

[25] KOPERSKI J., *Van der Waals Complexes in Supersonic Beams*, Wiley-VCH, Weinheim, 2003.

[26] KOPERSKI J., *Study of diatomic van der Waals complexes in supersonic beams*, Physics Reports **369**(3), 2002, pp. 177–326, and references therein.

[27] ŁUKOMSKI M., KOPERSKI J., CZUCHAJ E., CZAJKOWSKI M., *Structure of excitation and fluorescence spectra recorded at the $^1 0_u^+(5^1P)–X^1 0_g^+$ transition of Cd_2*, Physical Review A **68**(4), 2003, article 042508; *Erratum*, Physical Review A **69**(4), 2004, 049901.

[28] RUSZCZAK M., STROJECKI M., KOPERSKI J., *Short-range repulsion in the $D^1 0^+(^1\Sigma^+)$-state potential of the CdRG (RG = Ar,Kr) molecules determined from direct continuum←bound excitation detected at the $D^1 0^+←X^1 0^+(^1\Sigma^+)$ transition*, Chemical Physics Letters **416**(1–3), 2005, pp. 147–151.

[29] STROJECKI M., RUSZCZAK M., KROŚNICKI M., ŁUKOMSKI M., KOPERSKI J., *The $^3 0_u^+(4^3P_1)$- and $X 0_g^+$-state potential of Zn_2 obtained from excitation spectrum recorded at the $^3 0_u^+←X^1 0_g^+$ transition*, Chemical Physics **327**(2–3), 2006, pp. 229–236.

[30] ŁUKOMSKI M., STROJECKI M., RUSZCZAK M., KOPERSKI J., *Rotational structure of the $v' = 45 ← v'' = 0$ band of the $^1 0_u^+(5^1P_1)←X^1 0_g^+$ transition in $^{228}Cd_2$: direct determination of the ground- and excited-state bond lengths*, Chemical Physics Letters **434**(4–6), 2007, pp. 171–175; *Erratum*, Chemical Physics Letters **436**, 2007, p. 400.

[31] KOPERSKI J., RUSZCZAK M., STROJECKI M., ŁUKOMSKI M., *Spectroscopy of the $^1 1_u(5^1P_1)$ and $^1 0_u^+(5^1P_1)$ singlet electronic states of cadmium dimer: bond lengths and verification of ab initio potentials*, Journal of Molecular Spectroscopy **243**(2), 2007, pp. 134–141.

[32] KOPERSKI J., *Group-12 vdW dimers in free-jet supersonic beams: the legacy of Eugeniusz Czuchaj continues*, The European Physical Journal – Special Topics **144**(1), 2007, pp. 107–114.

[33] STROJECKI M., RUSZCZAK M., ŁUKOMSKI M., KOPERSKI J., *Is Cd2 truly a van der Waals molecule? Analysis of rotational profiles recorded at the $A 0_u^+$, $B 1_u←X 0_g^+$ transitions*, Chemical Physics **340**(1–3), 2007, pp. 171–180.

[34] STROJECKI M., KROŚNICKI M., KOPERSKI J., *Short-range repulsion in the $D^1\Sigma_0^+$-state potential of the ZnRg (Rg = Ne, Ar, Kr) complexes determined from direct free←bound excitation at the $D^1\Sigma_0^+ ←X^1\Sigma_0^+$ transition*, Chemical Physics Letters **465**(1–3), 2008, pp. 25–30.

[35] RUSZCZAK M., STROJECKI M., ŁUKOMSKI M., KOPERSKI J., *Potential energy curves for the $B^1 1_u$ state and short-range part of the $X^1 0_g^+$ state of Cd_2 determined from excitation and dispersed fluorescence spectra recorded using the $B^1 1_u ↔ X^1 0_g^+$ transition*, Journal of Physics B: Atomic, Molecular and Optical Physics **41**(24), 2008, article 245101.

[36] Strojecki M., Krośnicki M., Łukomski M., Koperski J., *Excitation spectra of CdRg (Rg = He, Ne, Xe) complexes recorded at the $D\,^1\Sigma_0^+ \leftarrow X\,^1\Sigma_0^+$ transition: from the heaviest CdXe to the lightest CdHe*, Chemical Physics Letters **471**(1–3), 2009, pp. 29–35.

[37] Strojecki M., Krośnicki M., Koperski J., *Repulsive and bound parts of the interatomic potentials of the lowest singlet electronic energy states of the MeRg complexes (Me = Zn, Cd; Rg = He, Ne, Ar, Kr, Xe)*, Journal of Molecular Spectroscopy **256**(1), 2009, pp. 128–134.

[38] Strojecki M., Koperski J., *LIF dispersed emission spectra and characterization of ZnRg (Rg = Ne, Ar, Kr) ground-state potentials*, Chemical Physics Letters **479**(4–6), 2009, pp. 189–194.

[39] Strojecki M., Krośnicki M., Zgoda P., Koperski J., *Characterization of bound parts of the $b\,^3 0_u^+(5\,^3P_1)$, $c\,^3 1_u(5\,^3P_2)$ and $X\,^1 0_g^+$ states of Cd_2 revisited: bound–bound excitation and dispersed emission spectra*, Chemical Physics Letters **489**(1–3), 2010, pp. 20–24.

[40] Urbańczyk T., Strojecki M., Koperski J., *Structure of vibrational bands of the $E\,^3\Sigma^+(6\,^3S_1) \leftarrow \leftarrow A\,^3\Pi_0^+(5\,^3P_1)$, $B\,^3\Sigma_1^+(5\,^3P_1)$ transitions in CdAr and CdKr studied by optical–optical double resonance method*, Chemical Physics Letters **503**(1–3), 2011, pp. 18–24.

[41] Koperski J., Strojecki M., Krośnicki M., Urbańczyk T., *Potentials of the $D\,^1 0_u^+(6\,^1S_0)$ and $F\,^3 1_u(6\,^3P_2)$ electronic Rydberg states of Cd_2 from ab initio calculations and laser-induced fluorescence excitation spectra*, Journal of Physical Chemistry A **115**(25), 2011, pp. 6851–6860.

[42] Ruszczak M., Strojecki M., Krośnicki M., Łukomski M., Koperski J., *Spectroscopy of Cd_2 and Zn_2 molecules in free-jet supersonic beams: Experimental and theoretical studies*, Optica Applicata **36**(4), 2006, pp. 451–459.

[43] Ming Yu, Dolg M., *Covalent contributions to bonding in group 12 dimers M_2 (Mn = Zn, Cd, Hg)*, Chemical Physics Letters **273**(5–6), 1997, pp. 329–336.

[44] Masnou-Seeuws F., Pillet P., *Formation of ultracold molecules (T ≤ 200 μK) via photo-association in a gas of laser-cooled atoms*, Advances in Atomic, Molecular, and Optical Physics **47**, 2001, pp. 53–127.

[45] Smalley R.E., Wharton L., Levy D.H., *Molecular optical spectroscopy with supersonic beams and jets*, Accounts of Chemical Research **10**(4), 1977, pp. 139–145.

[46] Lubman D.M., Rettner C.T., Zare R.N., *How isolated are molecules in a molecular beam?*, Journal of Physical Chemistry **86**(7), 1982, pp. 1129–1135.

[47] Urbańczyk T., Strojecki M., Krośnicki M., Koperski J., *Entangled atoms of cadmium: from production to tests of Bell's inequality*, Proceedings of the XLI Meeting of Polish Physicists, September 4–9, 2011, Lublin, Poland, p. 222.

[48] Strojecki M., *Rotational Spectra Simulator*, v. 1.6, 2007.

[49] Lukeš V., Ilčin M., Laurinc V., Biskupič S., *On the structure and physical origin of van der Waals interaction in zinc, cadmium and mercury dimers*, Chemical Physics Letters **424**(1–3), 2006, pp. 199–203.

[50] Leroy R.J., Kraemer G.T., *BCONT 2.2*, University of Waterloo Chemical Physics Research Report CP-650R2, 2004. The source code: http://leroy. uwaterloo.ca.

[51] Koperski J., Qu X., Meng H., Kenefick R., Fry E.S., *Rotational analysis of the (57, 0) band of the $D1_u \leftarrow X0_g^+$ triplet–singlet transition in Hg_2 produced in a free-jet expansion beam*, Chemical Physics **348**(1–3), 2008, pp. 103–112.

[52] Tellinghuisen J., [In] *Photodissociation and Photoionization*, Lawley K.P. [Ed.], Wiley and Sons, 1985, p. 299.

[53] Łukomski M., Koperski J., Czajkowski M., *Double-well potential energy curve of cadmium–krypton molecule in the $B1(5\,^3P_1)$ excited state*, Spectrochimica Acta A **58**(8), 2002, pp. 1757–1767.

[54] Koperski J., Czajkowski M., *Spectroscopical characterization of CdNe van der Waals complex in the $E1(^3\Sigma^+)$ Rydberg state*, Chemical Physics Letters **357**(1–2), 2002, pp. 119–125.

[55] Koperski J., Czajkowski M., *The structure of the lowest electronic Rydberg state of CdAr complex determined by laser double resonance method in a supersonic jet-expansion beam*, Spectrochimica Acta A **59**(11), 2003, pp. 2435–2448.

[56] KOPERSKI J., CZAJKOWSKI M., *Electronic structure of the CdKr lowest Rydberg state determined from laser-excitation spectra using supersonic beam and double optical resonance methods*, Physical Review A **69**(4), 2004, article 042509.

[57] KOSMAN W.M., HINZE J., *Inverse perturbation analysis: Improving the accuracy of potential energy curves*, Journal of Molecular Spectroscopy **56**(1), 1975, pp. 93–103.

[58] SCHAUTZ F., FLAD H.-J., DOLG M., *Quantum Monte Carlo study of Be_2 and group 12 dimers M_2 (M = Zn, Cd, Hg)*, Theoretical Chemistry Accounts **99**(4), 1998, pp. 231–240.

[59] DOLG M., FLAD H.-J., *Ground state properties of Hg_2. 1. A pseudopotential configuration interaction study*, Journal of Physical Chemistry **100**(15), 1996, pp. 6147–6151.

[60] KOPERSKI J., ATKINSON J.B., KRAUSE L., *The $0_u^+(6^3P_1)$–$X0_g^+$ spectrum of Hg_2 excited in a supersonic jet*, Chemical Physics Letters **219**(3–4), 1994, pp. 161–168.

[61] WALTHER TH., *Interactions in Ultracold Gases: From Atoms to Molecules*, Weidemüller M., Zimmermann C., [Eds.], Wiley-VCH, Weinheim, 2003, pp. 405–406.

[62] FRY E.S., WALTHER T., SHIFANG LI, *Proposal for a loophole-free test of the Bell inequalities*, Physical Review A **52**(6), 1995, pp. 4381–4395.

[63] URBAŃCZYK T., STROJECKI M., KROŚNICKI M., KOPERSKI J., *Entangled cadmium atoms – from the method of production to the test of Bell inequalities*, Optica Applicata **42**(2), 2012, pp. 433–441.

[64] AUTUMN K., YICHING A. LIANG, HSIEH S.T., ZESCH W., WAI PANG CHAN, KENNY T.W., FEARING R., FULL R.J., *Adhesive force of a single gecko foot-hair*, Nature **405**(6787), 2000, pp. 681–685.

[65] MURPHY M.P., SITTI M., *Waalbot: An agile small-scale wall-climbing robot utilizing dry elastomer adhesives*, IEEE/ASME Transactions on Mechatronics **12**(3), 2007, pp. 330–338.

[66] MURPHY M.P., KUTE C., MENGÜÇ Y., SITTI M., *Waalbot II: Adhesion recovery and improved performance of a climbing robot using fibrillar adhesives*, The International Journal of Robotics Research **30**(1), 2011, pp. 118–133.